QUENCH PERFORMANCE AND FIELD QUALITY OF 90-mm Nb_3Sn QUADRUPOLES OF TQC SERIES*

G. Chlachidze#, N. Andreev, R. Bossert, J. DiMarco, V.V. Kashikhin, M.J. Lamm, F. Nobrega, I. Novitski, M. Tartaglia, G. Velev, A.V. Zlobin, Fermilab, Batavia, IL 60510, U.S.A.

Abstract

Accelerator quality Nb_3Sn quadrupole models of TQC series have been fabricated and tested at Fermilab. The magnet design includes 90-mm aperture two-layer coils supported by a stainless steel collar, iron yoke and stainless steel skin. TQC models are the first Nb_3Sn quadrupoles using the collar-based structure. This paper describes the design and fabrication features of TQC quadrupole models with both traditional quadrupole-style and alternative dipole-style collars, and presents model test results, including quench performance and field quality at 4.5 K and 1.9 K.

INTRODUCTION

Fermilab is developing high-field dipoles and quadrupoles based on Nb_3Sn superconductor for the upgrades of the Large Hadron Collider (LHC) [1, 2] and other applications including Muon Collider Storage Ring [3]. Several technological quadrupole models of TQC series [4, 5] have been developed, fabricated and tested at Fermilab, utilizing recycled coils built by Fermilab and LBNL within the framework of the US LHC Accelerator Research Program (LARP). These models employ a conventional mechanical structure based on stainless steel collars similar to that used in NbTi accelerator magnets, in particular the MQXB quadrupoles [6] used in LHC IRs.

The collar has been a reliable structure, providing the required coil geometry and alignment as well as pre-stress and support. Although the design is well-established for NbTi magnets, the TQC models represent a first attempt to use a collar-based structure for Nb_3Sn coils. This paper describes the construction and testing of TQC03E, a 1 m long model with dipole style collars and RRP 108/127 strand. These results are compared with TQC02Ea/b, two earlier models using quadrupole and dipole style collars respectively [7].

TQC DESIGN AND FABRICATION

The traditional quadrupole collaring system uses quadrupole-symmetric collars. The collared coil assembly is compressed in a vertical four-jaw press, while a separate set of presses drives in keys to lock the collars together. Collars are compressed in discrete sections, each 10-15 cm long, proceeding in the longitudinal direction. For brittle Nb_3Sn coils, many passes are required to avoid large stress/strain variations at the transition between compressed and non-compressed sections. To limit the stress difference between adjacent sections to ~10-15 MPa, 6-8 passes are usually required to achieve the final target coil pre-stress.

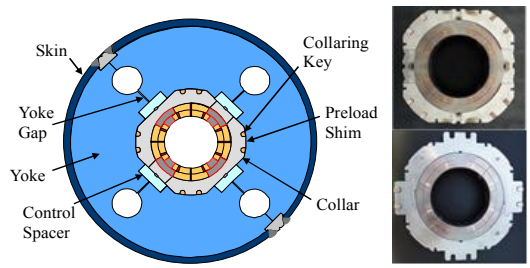

Figure 1: TQC with quadrupole and dipole style collars.

An alternative collaring system uses a dipole-symmetric collar. The coil assembly with such collars is compressed simultaneously along the entire length in a horizontal press, similar to superconducting dipoles, eliminating local stress gradients. This lowers the risk of Nb_3Sn coil damage resulting from incremental coil compression. A TQC cold mass with collars of both types are shown in Fig. 1. A detailed discussion of the design features and collaring methods for Nb_3Sn quadrupole magnets is presented in [8].

Quadrupole models discussed in this paper were built with coils previously used in LARP models of the TQS series [9]. The baseline TQ coil design and fabrication technology are described in [4]. The coils have titanium alloy poles. The cable was made using 0.7-mm diameter Nb_3Sn strand based on the Rod Restack Process (RRP) by Oxford Superconducting Technology, and a 125-μm thick S2-glass sleeve insulation [7, 9].

TQC models were assembled in two stages. The first stage includes coil collaring using collar packs. The second stage includes collared coil yoking and skinning. The collared coil provides an intermediate preload of 30-50 MPa, while additional pre-load from the yoke and skin through radial shims increases preload in the final assembly to 110-150 MPa. Coil over-compression during cool-down is prevented by the control spacer when using quadrupole style collars and by the collar surface for dipole style collars. TQC02Eb and TQC03E models also included a coil-to-collar alignment key. Coil combinations in TQC models, strand design and average coil pre-stresses after assembly are shown in Table 1.

Table 1: Design and assembly features of TQC models

Model	Coils	Strand design	Coil prestress, MPa (warm)
TQC02Ea	20,21,22,23	RRP-54/61	-112
TQC02Eb	20,28,22,23		-124
TQC03E	30,31,32,33	RRP-108/127	-118

* Work supported by Fermi Research Alliance, LLC, under contract No. DE-AC02-07CH11359 with the U.S. Department of Energy
# guram@fnal.gov

ISBN 978-3-95450-115-1

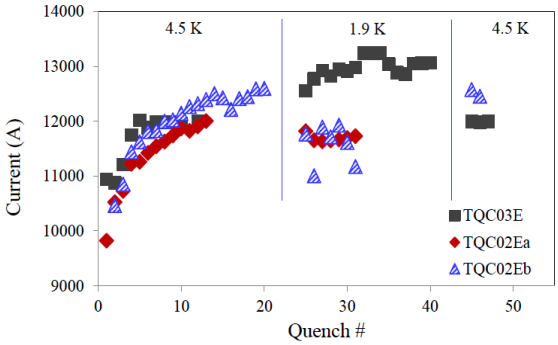

Figure 2: Magnet training quenches at 4.5 K and 1.9 K.

MAGNET PERFORMANCE

TQC models were tested in liquid helium at Fermilab's Vertical Magnet Test Facility. The magnet test plan included quench training and ramp rate dependence studies both at 4.5 K and 1.9 K, as well as temperature dependence study and field quality measurements. TQC03E was tested in February-March of 2012, the reference models TQC02Ea/b were tested in 2007 and 2010 respectively. TQC02Ea/b fabrication and test results were reported in [7].

Training quenches of TQC03E and TQC02Ea/b at 4.5 K and 1.9 K are shown in Fig. 2. At 4.5 K, after some training the quench current in TQC03E and TQC02Ea reached 12 kA, producing a field gradient of 200 T/m, while TQC02Eb reached 12.6 kA or 210 T/m.

At 1.9 K, TQC03E after training reached 13.2 kA or field gradient of 220 T/m, whereas TQC02Ea/b showed erratic quench performance related to flux jump instabilities in Nb_3Sn strands, which is typical for magnets with RRP-54/61 strand design. TQC03E training quenches mostly developed in the pole-turn blocks, but at the plateau quench location moved to the mid-plane blocks of the magnet.

TQC03E exhibited good training memory. After a full thermal cycle the magnet reached quench plateau without training at 4.5 K and with one training quench at 1.9 K (Fig. 3).

TQC03E quench performance is consistent with the test results of TQS03 assembled with the same coils using the aluminum shell structure (see Fig. 3). TQS03 was tested at CERN under various pre-stress conditions and degradation of the order of 5% was observed in quench performance after the coil pre-load reached ~200 MPa [9].

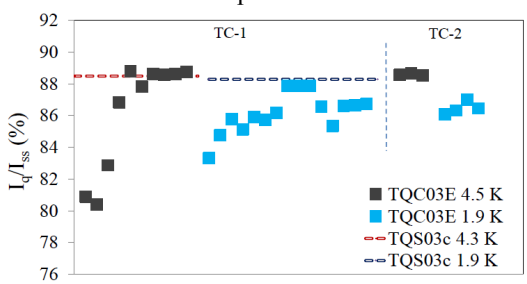

Figure 3: Training quenches normalized on magnet SSL.

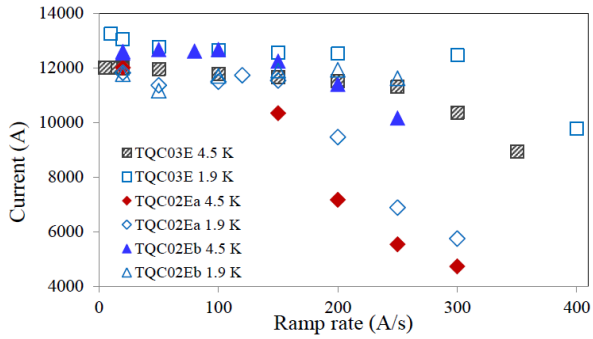

Figure 4: Quench current dependence on current ramp rate.

Magnet ramp rate dependences at 4.5 K and 1.9 K are shown in Fig. 4. All ramp rate quenches initiated in the mid-plane blocks. While the high ramp rate quenches in the mid-plane turns are caused by eddy current losses in the cable, the low ramp rate quenches in the low field area are likely due to the flux jump instabilities. At 1.9 K the flux jump related quenches in TQC02Eb are seen at ramp rates up to 200 A/s. At 4.5 K they occur at ramp rates up to 100 A/s and at currents only a few percent lower than the coil short sample limit (SSL). TQC02Eb quench current at 1.9 K is even less than at 4.5 K for ramp rates below 150 A/s. Similar features are seen in the ramp rate dependence of TQC02Ea (see Fig. 4).

The temperature dependence of the quench current at a ramp rate of 50 A/s is shown in Fig. 5. TQC03E shows expected monotonic increase of quench current with temperature decrease whereas TQC02Eb quench performance clearly is affected by the flux jump instabilities at temperatures below 3.5 K. After training at ~3.2 K it reached the maximum field gradient of 217 T/m.

The conductor residual resistivity ratio (RRR) was measured for all coils in the magnet. The average RRR for the inner and outer layers in TQC03E are 170 and 182 respectively. The measured variations of RRR for the reference models were 209-230 in TQC02Ea and 200-210 in TQC02Eb. Rather low RRR in TQC03E could be caused by high coil pre-loads (up to 200 MPa) applied in TQS03.

Table 2 summarizes the average harmonics for TQC03E, TQC02Ea and TQC02Eb at a field gradient of 100 T/m. One can see that the magnetic measurements in models with dipole-style collar do not show any specific distortions related to the collar design.

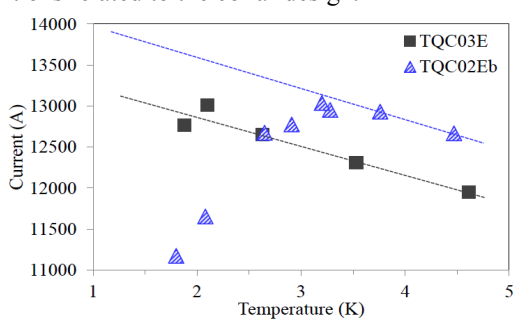

Figure 5: Quench current at different bath temperatures.

Table 2: Average body harmonics (in units, where 1 unit is equal to 10^{-4} of the main field) at 100 T/m

n	b_n			a_n		
	02Ea	02Eb	03E	02Ea	02Eb	03E
3	-2.56	-3.57	-0.5	1.72	4.71	-2.64
4	-1.65	-3.34	0.19	-2.7	-0.29	-2.81
5	0.72	0.20	-0.03	1.61	-0.76	2.21
6	-0.96	-0.62	0.72	0.59	0.05	-0.36
7	-0.34	0.03	-0.06	-0.32	0.10	0.18
8	0.14	-0.07	-0.06	-0.07	0.01	-0.08
9	0.06	0.06	0.14	0.12	-0.02	0.01
10	-0.08	0.01	-0.02	-0.01	0.02	0.08

The conductor magnetization and iron saturation effect on magnet transfer function (TF) and normal dodecapole (b_6) are shown in Figs. 6 and 7. The iron saturation effect is small and consistent with the calculations.

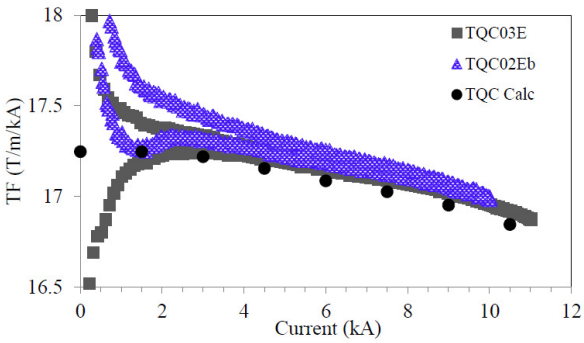

Figure 6: Transfer function (G/I) vs. magnet current.

The hysteretic behaviors of magnet TF and b_6 are proportional to the filament diameter (D_{eff}) and the critical current density $J_c(B)$ of the superconducting strand. The smallest hysteresis is observed in TQC03E made of RRP-108/127 strand. D_{eff} in 0.7 mm round strand is ~40 μm for this design and ~60 μm for the RRP 54/61 strand design.

No long-term dynamic effects (decay and snap-back) were found in the allowed harmonics.

CONCLUSION

TQC quadrupole models with quadrupole and dipole style collar designs were successfully built and tested at Fermilab. Magnets with the dipole style collars achieved the same coil preloads as those using the traditional quadrupole style collars, but with significantly shorter assembly time and reduced risk of coil damage.

The dipole-style collar design and new collaring technique used in TQC03E and TQC02Eb did not introduce any additional degradation in magnet performance. Field quality of TQC02Ea and TQC02Eb, the two magnets with the same coils but different collar design, are also consistent. Harmonic measurements do not show any significant anomalies related to the dipole style collar design. Quench performance of TQC models is consistent with the test results of the same coils in a shell-based TQS structure. TQC tests after multiple handling and test cycles once again confirmed the robustness of Nb_3Sn coils.

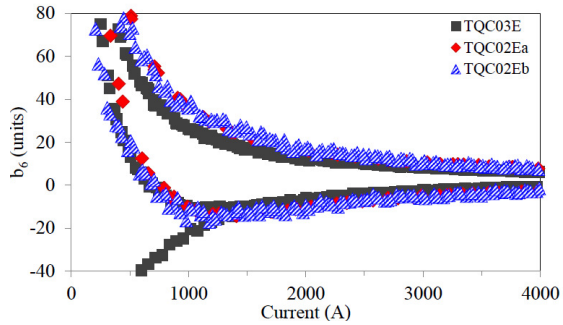

Figure 7: b_6 vs. magnet current.

The TQC program at Fermilab has demonstrated that the yoke-supported collar structure can be used with brittle Nb_3Sn coils. The dipole style collars can be easily adopted for long Nb_3Sn coils, making this approach very efficient for future LHC upgrades. NbTi coils could be replaced with Nb_3Sn coils in the same mechanical structure to increase magnet aperture and temperature margin, reduce magnet length, or provide any combination of these features.

ACKNOWLEDGMENT

The authors thank the technical staff of Fermilab's Technical Division for their contributions to magnet fabrication and test, and LARP for providing coils.

REFERENCES

[1] A.V. Zlobin et al., "Large-Aperture Nb_3Sn Quadrupoles for 2nd generation LHC IRs", Proceedings of EPAC 2002, Paris, June 3-7 2002, pp.2451-2453

[2] A.V. Zlobin et al., "Development of Nb_3Sn 11 T Single Aperture Demonstrator Dipole for LHC Upgrades", Proceedings of PAC 2011, New-York, March 2011, pp. 1460-1462

[3] A.V. Zlobin et al., "Magnet Designs for Muon Collider Ring and Interaction Regions", Proceeding of IPAC 2010, Kyoto, Japan, May 2010, pp. 388-390

[4] R.C. Bossert et al., "Development of TQC01, a 90mm Nb_3Sn Model Quadrupole for LHC Upgrade Based on SS Collar," *IEEE Trans. on Applied Supercond.*, vol. 16, no. 2, pp. 370-373, June 2006

[5] R. Bossert et al., "Fabrication and Test of LARP Technological Quadrupole Models of TQC series," *IEEE Trans. on Applied Supercond.*, vol. 19, no. 3, pp. 1226-1230, June 2009.

[6] R. Bossert et al., "Development of a High Gradient Quadrupole for the LHC Interaction Regions", *IEEE Trans. on Applied Supercond.*, vol. 7, no 2, pp. 751-754, June 1997.

[7] R. Bossert et al., "Fabrication and Test of 90-mm Nb_3Sn Quadrupole Model Based on Dipole-type Collar", *IEEE Trans. on Applied Supercond.*, Volume 21, No 3, pp. 1777-1780, June 2011.

[8] R. Bossert et al., "Development and Test of Collaring Methods for Nb_3Sn Quadrupole Magnets", Transactions of the CEC, Tucson, AZ, June 2009, pp. 507-514.

[9] H. Felice et al., "Performance of a Nb_3Sn Quadrupole Under High Stress", *IEEE Trans. on Applied Supercond.*, Vol. 21, No 3, pp. 1849-1853, June 2011.

ISBN 978-3-95450-115-1